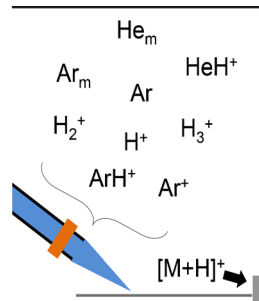# The Effects of Added Hydrogen on Noble Gas Discharges Used as Ambient Desorption/Ionization Sources for Mass Spectrometry

Wade C. Ellis, Charlotte R. Lewis, Anna P. Openshaw, Paul B. Farnsworth

Department of Chemistry and Biochemistry, Brigham Young University, Provo, UT 84602, USA

Abstract. We demonstrate the effectiveness of using hydrogen-doped argon as the support gas for the dielectric barrier discharge (DBD) ambient desorption/ionization (ADI) source in mass spectrometry. Also, we explore the chemistry responsible for the signal enhancement observed when using both hydrogen-doped argon and hydrogen-doped helium. The hydrogen-doped argon was tested for five analytes representing different classes of molecules. Addition of hydrogen to the argon plasma gas enhanced signals for gas-phase analytes and for analytes coated onto glass slides in positive and negative ion mode. The enhancements ranged from factors of 4 to 5 for gas-phase analytes and factors of 2 to 40 for coated slides. There was no significant increase in the background. The limit of detection for caffeine was lowered by a factor of 79 using H_2/Ar and 2 using H_2/He. Results are shown that help explain the fundamental differences between the pure-gas discharges and those that are hydrogen-doped for both argon and helium. Experiments with different discharge geometries and grounding schemes indicate that observed signal enhancements are strongly dependent on discharge configuration.

Keywords: Ambient desorption/ionization, Hydrogen addition, Dielectric barrier discharge

Introduction

The introductions of desorption electrospray ionization (DESI) [1] and direct analysis in real time (DART) [2] in 2005 have led to explosive growth in the field of ambient desorption/ionization mass spectrometry. Of particular interest have been the plasma-based ADI sources [3–5] that require little to no sample preparation, enable fast analysis times, and feature simple source construction [6, 7]. Plasma-based ADI sources usually use helium for the plasma gas because of its high ionization potential and the high energies of its metastable states, but other plasma gases have been utilized, including argon, nitrogen, and air [3, 8]. However, little work has been done to determine the effectiveness of using gas mixtures as plasma gases for these ADI sources. Given that the predominant analyte ions formed when using these sources are $[M + H]^+$ ions, the most attractive dopant gases would be hydrogen

donors. The simplest hydrogen source is molecular hydrogen. Previous work in our laboratory [9, 10] has shown the benefits of using hydrogen-doped helium as the plasma gas for a high-frequency dielectric barrier discharge (DBD) source. These benefits included enhanced signals and faster desorption rise times. Our experiments with hydrogen-doped helium plasmas also pointed to a change in the desorption mechanism with the addition of hydrogen.

The widespread use of helium as the support gas for plasma-based ADI sources has presented some significant problems for users. Helium is expensive, non-renewable, and it strains vacuum systems. Based on cost and availability, argon would seem to be a good alternative to helium. However, experiments with pure argon discharges have yielded sensitivities 10–100 times worse than those recorded with helium plasmas using the LTP [8]. There is good reason to think that adding hydrogen to argon could improve its performance as an ADI plasma gas. The effects of hydrogen on argon plasmas have been studied extensively by researchers in the field of inductively coupled plasma mass spectrometry (ICP-MS) [11–15]. Hydrogen has been found to be an effective way to remove argon ions from the ion beam in ICP-MS. They undergo rapid and efficient reactions with molecular hydrogen resulting in the formation of

Correspondence to: Paul B. Farnsworth; *e-mail:* paul_farnsworth@byu.edu

ions such as ArH^+, ArH_2^+, H_2^+, and H_3^+ [11, 13]. Of these ions, H_3^+ is the most abundant. These ions, especially H_3^+ and ArH^+, could react readily with analyte ions to produce $[M + H]^+$ ions suitable for detection in a mass spectrometer. It has been observed that the main water cluster ion present in radio frequency (rf) plasma discharges is the $H(H_2O)_4^+$ ion [16]. The proton affinities of Ar, H_2, and $(H_2O)_4$ are 369.2 kJ mol^{-1}, 423.8 kJ mol^{-1}, and 933 kJ mol^{-1}, respectively [17–19], suggesting that the ArH^+ and H_3^+ ions could act as more versatile proton donors than $H(H_2O)_4^+$ in an ADI source. The proton affinities of different order water clusters are similarly higher than those of ArH^+ and H_3^+. We present here experimental characterization of a hydrogen-doped argon plasma as an ADI source for mass spectrometry.

It has been brought to our attention by two research laboratories through private communication that the results reported previously showing signal enhancement with hydrogen-doped helium [9] have not been successfully reproduced in their labs. They report using different types of mass spectrometers with presumably different voltage settings that did not exactly correspond to those used in our lab. However, we have continued to see the effect in the studies we have performed. One purpose of this paper is to detail those circumstances under which the signal enhancement occurs and does not occur such that the results may be more successfully reproduced in other laboratories.

Experimental

Chemicals

The chemicals used in this study were chosen to match previous studies [9, 10, 20, 21] done with pure helium and hydrogen-doped helium. They included caffeine (Sigma Aldrich, Steinheim, Germany), diphenylamine (Brigham Young University chemical surplus, source unknown), anthracene (Spectrum Chemical Mfg. Corp., Gardena, CA, USA), coumarin 460 (Exciton, Dayton, OH, USA), and 1,3-dinitrobenzene (The Matheson Company, East Rutherford, NJ, USA). HPLC grade methanol (Sigma Aldrich, St. Louis, MO, USA) was used to create all of the solutions used in this study for coating glass slides. HPLC grade acetonitrile (Fisher Chemical, Waltham, MA, USA) was used in the experiments determining the limit of detection for caffeine.

Dielectric Barrier Discharge

The dielectric barrier discharge (DBD) used has been described previously [22]. A brief description will be provided here. The discharge was created in a fused quartz capillary (3 mm o.d., 1 mm i.d., 68 mm long) between a grounded needle electrode inside the capillary and a copper ring electrode (7 mm o.d., 3 mm i.d., 3 mm long) attached to the outside of the capillary. The copper ring electrode was secured to the capillary 1 cm from the end. The distance between the needle electrode and the ring electrode was 10 mm when using argon and 42 mm when using helium. A 1/8-inch stainless steel Swagelok-T was

used to connect the discharge components. The support gases used were ultra-high purity argon, 2.90% hydrogen in argon, ultra-high purity helium, and 1.0% hydrogen in helium. All gases were obtained from Airgas (Radnor, PA, USA); 2.90% hydrogen in argon was used instead of any higher hydrogen concentration to avoid treating the mixture as a flammable gas. The flow rate for all plasma gases was 2 L min^{-1}. Flow rates were controlled by a pair of MKS1170A mass flow controllers with MKS246C power supplies/readouts (MKS Instruments, Andover, MA, USA). Power was supplied to the copper ring electrode with an ENI HPG-2 rf power supply (MKS Instruments, Andover, MA, USA). Under these conditions, the plasma plume protruded approximately 5 mm past the tip of the capillary for argon and 2 cm for helium.

AC Discharge

The AC discharge used herein has also been described previously [22]. Briefly, a glass tube (6.3 mm o.d., 3.8 mm i.d.) had a coaxial tungsten pin electrode (1 mm o.d.) to which high voltage was applied, and a grounded copper plate (9.8 mm diameter) with a 2 mm hole coaxial with the tube and tungsten pin was attached to the end of the glass tube. Thus, the discharge operated in a pin-to-plate mode. The distance between the tungsten pin and the coper plate was 4 mm. Power was applied to the tungsten pin using the same HPG-2 power supply used for the DBD. The power applied was 10 W at 350 kHz. Gas was supplied at a rate of 2 L min^{-1} using one of the MKS1170A mass flow controllers with its corresponding power supply.

Mass Spectrometer Setup

Mass spectra were collected using a MicrOTOF II (Bruker Daltonics, Billerica, MA, USA) time-of-flight mass spectrometer. MicrOTOF Control 3.0 software was used for instrument control and data acquisition, and DataAnalysis 4.0 software was used to process the acquired spectra.

The mass spectrometer was modified in the two ways. First, the electrospray ionization (ESI) source and the spray shield were removed so that the atmospheric pressure inlet was exposed. Second, an extra mechanical vacuum pump was attached to the first vacuum stage to reduce strain on the vacuum system when helium is used as the plasma gas. The extra pump was operational during all experiments regardless of plasma gas to maintain consistent vacuum conditions. The mass spectrometer operating parameters are presented in detail in Table 1.

Analyte was introduced into the mass spectrometer as illustrated schematically in Figure 1. First, to introduce analyte into the mass spectrometer in a way that allowed both desorption and ionization to occur, a glass slide was dipped in 25 mL of 100 ppm analyte-containing solution and withdrawn at a rate of 0.5 cm s^{-1} to reproducibly and uniformly coat the slide with target molecules. For 1,3-dinitrobenzene, a 1000 ppm solution was used to coat the slides. At this withdrawal rate, a 100 ppm solution has been shown to coat a slide with 0.44 ng cm^{-2} of rhodamine-6G [23]. This coating was found to be uniform over

Table 1. Mass Spectrometer Parameters for Positive Ion Mode. In Negative Ion Mode, the Polarities of the Appropriate Voltages (e.g., capillary, skimmer cones) Were Reversed

Parameter	Value
End plate offset	500 V
Capillary	−500 V
Dry gas flow rate	4.0 L/min
Dry gas temperature	250 °C
Acquisition rate	10.0 Hz
Rolling average	2.0
Capillary exit	140.0 V
Skimmer 1	46.7 V
Hexapole 1	23.0 V
Hexapole rf	100.0 V_{p-p}
Skimmer 2	23.3 V
Lens 1 transfer	37.6 µs
Lens 1 pre pulse storage	1.0 µs

the entire surface when viewed using fluorescence spectroscopy in the reference cited. The slide dipping apparatus was controlled using LabVIEW (National Instruments, Austin, TX, USA).

Once coated, the slide was placed horizontally in front of the mass spectrometer inlet. An x, y, z, θ stage was used to position the DBD above the slide at an angle of 35°. The tip of the DBD capillary was positioned 1.5 mm above the slide and 14 mm away from the mass spectrometer when using argon (Figure 1a), and 5 mm above the slide and 21 mm away from the inlet when using helium (Figure 1c). The AC discharge was also placed above the slide at an angle of 35°. The discharge was positioned 10 mm from the inlet of the mass spectrometer

and 1 mm above the slide. These parameters were chosen to give the most intense signal at the mass spectrometer. Spectra were recorded for 120 s.

The second sample introduction method was used to introduce sample into the mass spectrometer in a way that eliminated the desorption step. Gaseous sample was transported to the inlet by flowing dry nitrogen (AirGas) over solid sample contained in a three-neck round bottom flask at a flow rate of 200 mL/min. The flow rate of the nitrogen was controlled using a flow meter calibrated for air. The solid sample was heated by a 100 °C sand bath. The gas swept gaseous molecules out of the head space of the flask to the inlet of the mass spectrometer using 1/8 inch polypropylene tubing. The plastic tubing position was controlled by an x, y, z, θ stage (Thorlabs, Newton, NJ, USA).

The DBD or AC discharge was positioned pointing directly at the inlet of the instrument at a distance of 10 mm from the inlet when using argon (Figure 1b). When using helium, neither discharge could be pointed directly at the inlet without over-pressurizing the vacuum system of the mass spectrometer and causing it to shut down. Therefore, the discharges were placed at an angle in front of the mass spectrometer such that signal could still be obtained without the main helium stream entering the mass spectrometer (Figure 1d). All power, frequency, and flow rate settings were the same as in the coated slide experiments. As sample flowed with the discharge active, the support gas was switched between pure and hydrogen-doped gas using the mass flow controllers while spectra were recorded.

The power applied to the DBD was measured at 1.47 W for the argon discharge and 2.71 W for the H_2/Ar discharge at a
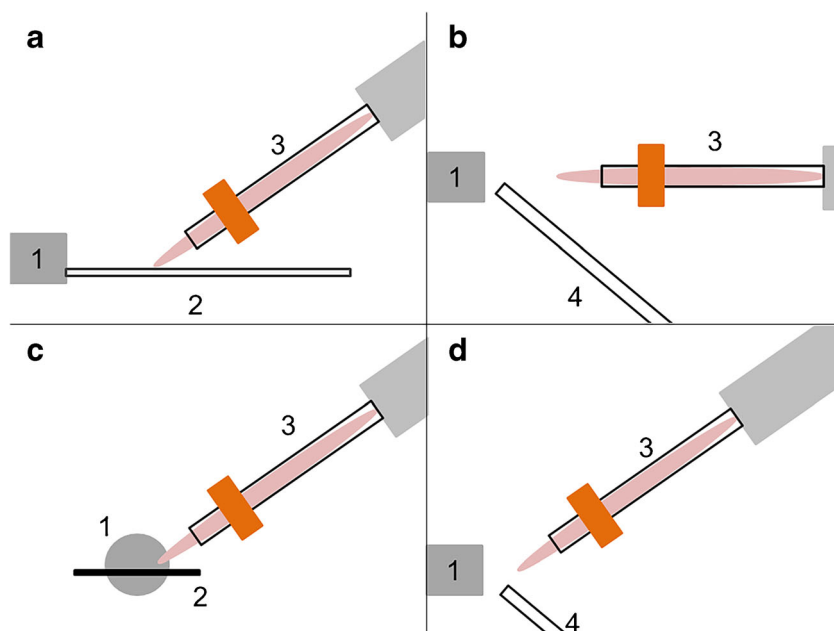

Figure 1. Experimental setup for each experiment described. **(a)** Side view of the coated slide setup when using Ar or H_2/Ar. **(b)** Side view of the gaseous analyte setup when using Ar and H_2/Ar. **(c)** View looking straight on the MS inlet of the coated slide setup when using He or H_2/He. Note that the discharge is perpendicular to the orientation used with Ar. **(d)** Side view of the gaseous analyte setup using He or H_2/He. The numbers represent the following: 1 – MS inlet, 2 – glass microscope slide coated in analyte, 3 – discharge (either DBD or AC glow discharge), and 4 – tube used to introduce gaseous caffeine

load power setting of 10 W on the power supply. The forward power at this setting was 25 W. For helium and H_2/He, the power was measured at 1.53 W and 0.32 W, respectively at a load power setting of 31 W. The frequency was 325 kHz for all gases. The power measurements were made by monitoring the voltage output of the power supply while monitoring the current using a current transformer (CT-2; Tektronix, Inc., Beaverton, OR, USA). The current and voltage waveforms were multiplied to get the power. The cause for the large differences between load and applied powers is the loss of power to the impedance matching network of the power supply. These settings were chosen to provide the most stable discharge and to minimize the difference between the load and forward powers.

Signal enhancements were calculated as the ratio of the signal produced by the hydrogen-doped discharge to the signal produced by the pure noble gas discharge. In the case of the gaseous sample introduction, the signal was the average steady-state value. For the samples deposited on slides, the signal was the integral of the selected ion count over the duration of the acquisition, 1–2 min.

Thermal Images

Thermal images were taken of a glass microscope slide under the active discharge using a thermal camera (Ti27; Fluke, Everett, WA, USA). The emissivity setting (ε) was 0.95 with a background setting of 20.0 and transmission of 100%. For each image, the slide temperature was monitored until it reached a consistent temperature before the image was taken. The temperature was reported at center of the area heated by the discharge.

Determination of the Optimal Amount of Hydrogen in Argon

To determine if there was an optimum amount of hydrogen for signal enhancement, separate mass flow controllers were attached to the argon and argon/hydrogen gas cylinders. The outputs came together to a single tube before going to the discharge. The mass flow controllers were used to vary the concentration of hydrogen in the plasma between 0% and 2.90%. Gaseous analyte was introduced with the DBD positioned 10 mm away from the MS inlet, and the concentration of H_2 that yielded the highest raw averaged signal was considered to be the best hydrogen concentration. Signal was acquired at each percentage of H_2 for 90 seconds.

Determination of the Limits of Detection

To determine the limits of detection for the gases used, series of solutions were created of caffeine in acetonitrile to obtain concentrations that covered at least three decades in concentration above the minimum detectable quantity. The actual ranges used depended on the gas composition in the discharge. Three µL volumes of these solutions were placed on a glass slide using a micropipette, allowed to dry, and placed in front of the

mass spectrometer. This allowed a known amount of analyte to be placed on the slide and removed by the plasma. Acetonitrile was used as the solvent instead of methanol because it formed a better bead of liquid on the surface of the hydrophilic slide, which allowed for more precise placement and containment of the droplet while still easily dissolving the caffeine.

For these experiments, the argon DBD was placed in the same configuration as for the coated slide experiments. The helium DBD was placed perpendicular to the axis of the mass spectrometer inlet so that the stream of helium did not disrupt the vacuum system. For helium, the discharge was placed 12 mm above the slide, 10 mm away from the inlet, and 7 mm off center at an angle of 45° relative to the glass slide. The inlet capillary voltage was increased from 500 to 1000 V for the helium experiments.

The signal was integrated over 1 min. The LOD was determined by multiplying the standard deviation of the blank replicates by 3 and dividing the results by the slope of the calibration curve. Blank measurements were taken of 3 µL of acetonitrile placed on the slide and allowed to dry.

Determination of the Area of Glass Slide Sampled by Plasma

To observe any correlation between the sensitivity of the source and the amount of analyte sampled, we determined what area of the slide was affected by the plasma while being analyzed. To do this, a 1000 ppm solution of coumarin 460 was made, and several slides were coated. The slides were then exposed to the DBD plasma for 30 s. Two slides were exposed to each support gas and the results averaged. Coumarin 460 is a dye that absorbs light strongly in the range of 365 to 375 nm, and subsequently fluoresces with a peak at 460 nm. The coated slides were bathed in light from a UV lamp, and non-fluorescent areas indicated where dye had been removed from the surface by the plasma. The non-fluorescent area was then measured with a ruler to approximate the sampled area.

Grounding Experiments

In order to observe the effects of alternate grounding pathways on the signal enhancement while using hydrogen-doped gases, a grounded nichrome wire was placed in the path of the DBD. The experiments using gaseous caffeine were then repeated, with the caffeine being introduced downstream of the wire. This was done for both the argon and helium DBDs.

These experiments were also repeated while applying a voltage to the wire using a DC power supply (Model IP-17; Heathkit, Santa Cruz, CA, USA). A resistor (3.3 kΩ) and capacitor (20 µF) in series with the wire isolated the applied voltage from ground. Positive and negative voltages were applied to the wire in separate experiments.

Background Ion Mass Spectra

The background ions emitted from each source were detected for the different plasma gas compositions to observe the

differences caused by hydrogen addition. To do this, the discharge was directed at the MS inlet as described in the gaseous analyte experiments except no gaseous analyte was introduced. The parameters of the mass spectrometer were changed as follows: hexapole rf from 100.0 to 5.0 V_{p-p}, lens 1 transfer from 37.6 to 11.0 µs. The observable mass range was thus extended down to 30 m/z.

Atomic Absorption Measurements of Helium Metastable Atoms

Measurements of the absolute number densities of helium metastable atoms (He_m) were taken with and without the grounded wire in place. The spectrometer used has been described previously [22]. In brief, a tunable diode laser (TLB-6900 VortexTM II; New Focus, Santa Clara, CA, USA) with a nominal wavelength of 1083 nm was used to excite three transitions between 1082.85 and 1083.15 nm from the He 2s $^3S_1$ state to the 2p $^3P_0$, $^3P_1$, or $^3P_2$ states. An InGaAs photodiode (SM05PD5A; ThorLabs, Newton, NJ, USA) was used as the detector. The signal was amplified using a differential amplifier (AM501; Tektronix, Beaverton, OR, USA), and data were collected using a digital oscilloscope (Wavesurfer; LeCroy, Chestnut Ridge, NY, USA). For detailed information on the spectrometer setup and how the number densities were calculated, please refer to reference 22.

Results and Discussion

Optimal Amount of Hydrogen in Argon

By performing experiments with differing ratios of hydrogen in argon, we were able to ascertain the best point at which to perform other analyses. As can be seen from the data presented in Figure 2, the signal increased for caffeine until approximately 1.5% hydrogen, after which a plateau of enhancement was reached. For anthracene, the signal increased gradually throughout the range of concentrations tested, reaching a maximum value at 2.9% H_2. Finally, the coumarin 460 signal plateaued initially like the caffeine signal, but then fell off at H_2 percentages above 2.2. The lack of a plateau in the anthracene data emphasizes that the enhancement of M^+ ion of anthracene by the addition of hydrogen proceeds by a different mechanism than the enhancement of the $[M + 1]^+$ ions of caffeine and coumarin 460. Based on these data, the remaining experiments were performed at 2.90% hydrogen so that only one mass flow controller was required. Diphenylamine was not included in these experiments because it is thermally labile and decomposition of the gaseous analyte before it reached the discharge muddled the results.

It should be noted that the optimal amount of hydrogen may vary as operating parameters such as power, frequency, source configuration, and source geometry relative to the mass spectrometer change [9].
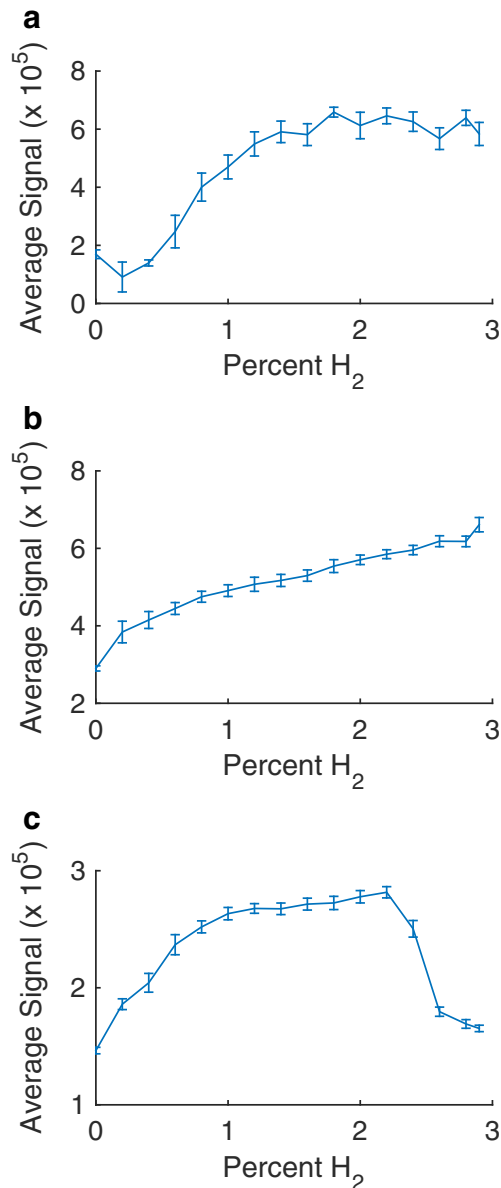

Figure 2. Mass spectrometric signal intensities for different percentages of hydrogen in argon for **(a)** caffeine, **(b)** anthracene, and **(c)** coumarin 460. For **(a)** and **(c)**, the traces are of the $[M + H]^+$ peak. For **(b)** the trace is of the M^+ peak. The error bars are the standard deviations of sixty one-second integrations, and are indicative of the short-term stability of the signal. Each curve was measured twice to check the reproducibility of the shape

Coated Slide Experiments

Dielectric Barrier Discharge The chronograms for the four analytes tested using the coated slide setup in positive ion mode are presented in Figure 3. The $[M + H]^+$ peak was monitored for caffeine, diphenylamine, and coumarin 460. The M^+ peak was monitored for anthracene. The m/z ratios monitored for caffeine, anthracene, diphenylamine, and coumarin 460 were 195.09, 178.23, 170.23, and 232.30, respectively, in positive ion mode. The signal enhancements were approximately six times for caffeine, two times for anthracene, three times for
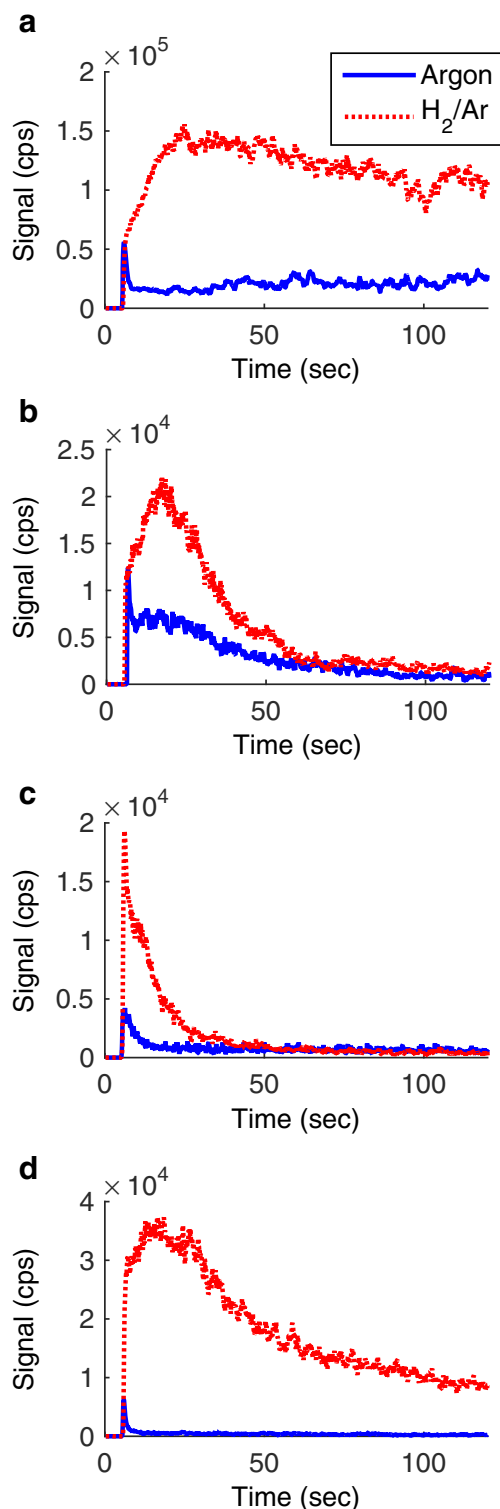
Figure 3. Chronograms for **(a)** caffeine, **(b)** anthracene, **(c)** diphenylamine, and **(d)** coumarin 460. For **(a)**, **(c)**, and **(d)**, the traces are of the $[M + H]^+$ peak. For **(b)** the trace is of the M^+ peak. Zero time is the beginning of data acquisition. The plasma was ignited at 6 s

$H]^+$ ions and those that produce M^+ ions, it appears that the addition of hydrogen influences both the mechanism that ionizes via proton addition and the one that ionizes via charge transfer.

In negative ion mode, the peaks observed for 1,3-dinitrobenzene were $[M - H + O]^-$ (183.00 m/z) and $[M]^-$ (168.01 m/z), with the peak at 183 m/z being most abundant. As reported in reference 9, no signal enhancement was observed of the peaks when using H_2/He. In fact, the signal when using H_2/He was lower than that obtained when using pure helium by a factor of 5. However, when using H_2/Ar, a signal enhancement of six times over that of pure argon was observed based on the integrated signal of the 183 m/z peak. This suggests that the addition of hydrogen to helium quenches or removes the species responsible for generating negative ions. The opposite appears to be true of hydrogen-doped argon.

As was the case with the helium plasma gas, the addition of hydrogen to argon alters the temporal desorption profile of most analytes. The sharp peak corresponding to plasma ignition disappears and the signal peaks later in time. The dramatic changes in temporal profiles with changes in gas composition, also seen with the addition of H_2 to He [9], suggest that the analyte molecules are not simply desorbed by heating up the glass substrate. Thermal images of glass slides exposed to the discharge add evidence that there is a non-thermal component of the desorption process. The temperature data are summarized in Table 2. The temperature of the slide exposed to the argon discharge was cooler than that of the H_2/Ar discharge. However, the opposite was true of the He and H_2/He plasma with the latter gas composition giving a lower slide temperature. There is no correlation between the measured surface temperature and either the signal level or signal rise time [9]. The data do not indicate what the non-thermal process may be. Possibilities include chemical sputtering and field desorption.

For some analytes, the absolute intensity of the analyte signal in H_2/Ar is comparable to that in helium. For slides dipped in 100 ppm caffeine in methanol solution, both hydrogen/argon and helium are in the range of 10^5 counts per second. Not all analytes perform comparably, but there is a significant improvement for all analytes over pure argon when using H_2/Ar. H_2/He is still far superior in terms of absolute signal intensity than either helium or H_2/Ar.

As noted in the Experimental section, the power applied to the discharge changes with the addition of hydrogen. For H_2/Ar, the power is higher than that of pure argon at the same settings, as noted in the Experimental section. The reverse is true for the H_2/He and helium DBDs. Although the power increase for the

diphenylamine, and 40 times for coumarin 460 in positive ion mode using the integrated signals. Because the hydrogen addition enhanced the signal for both molecules that produce $[M +$

Table 2. Temperatures Obtained from Thermal Images of Slides Exposed to the Plasma

Plasma Gas	Slide temperature (°C)
Argon	35.2
H_2/Ar	43.5
Helium	101.1
H_2/He	82.1

argon and H_2/Ar DBD's may account for some of the signal increase, we do not believe it is responsible for all of it due to the signal enhancement observed with the H_2/He discharge with its corresponding decrease in power compared to pure helium.

AC Discharge   The AC discharge gave signal comparable to the argon DBD for the $[M + H]^+$ peak of gaseous caffeine. However, when using the H_2/Ar gas with samples deposited on glass slides, no signal enhancement was observed.

Limits of Detection

The addition of hydrogen to plasma gas increases the sensitivity of the DBD source without proportional increases in the background. Under our experimental conditions, the absolute limits of detection obtained for caffeine were 18 ng and 230 pg for argon and H_2/Ar and 290 pg and 150 pg for the helium and H_2/He gases. The determined detection limits are within the range of those found for several compounds using the He LTP. Detection limits for the He LTP have been found to be in the range of 30 pg to 30 ng in a study from the Cooks laboratory [24]. The analytes tested in their study included amphetamine, benzoylecgonine, caffeine, cannabidiol, cocaine, codeine, diazepam, ephedrine hydrochloride, heroin, ketamine, methadone, methamphetamine, morphine, and tetrahydrocannabinol. Specifically, the limit of detection for caffeine was found to be 90 pg in that study. Although the limit of detection using H_2/Ar DBD is not as low as that found for the He LTP, there is an obvious improvement in limit of detection with the addition of hydrogen for both argon and helium.

Sample Area Versus Sensitivity

From the experiments to determine the size of the area sampled by each support gas when using the DBD, we observed that the argon plasma sampled an area on the slide of ~1.1 cm^2. The $H_2/$Ar plasma sampled an area of ~0.77 cm^2. The same discharge geometry was used in both cases. The sampled areas of the helium-based discharges were also determined. For helium and H_2/He, areas of ~1.85 cm^2 and ~1.14 cm^2 were sampled, respectively. For both noble gases, the more sensitive hydrogen-doped plasma sampled a smaller area of the slide. The hydrogen-doped plasmas appear to generate more analyte ions from a smaller sample.

Gas Phase Analyte Experiments

DBD   The results of the experiments in which caffeine and anthracene were introduced as a gas into the DBD are presented in Figure 4. Addition of hydrogen increased the signals by a factor of 5 for caffeine and 4 for anthracene. These gas-phase experiments and the data presented in Figure 2, combined with the measurements of sampled area, indicate that the major source of signal enhancement is in the gas-phase chemistry for caffeine and anthracene, and not in the desorption process. In contrast, the change in
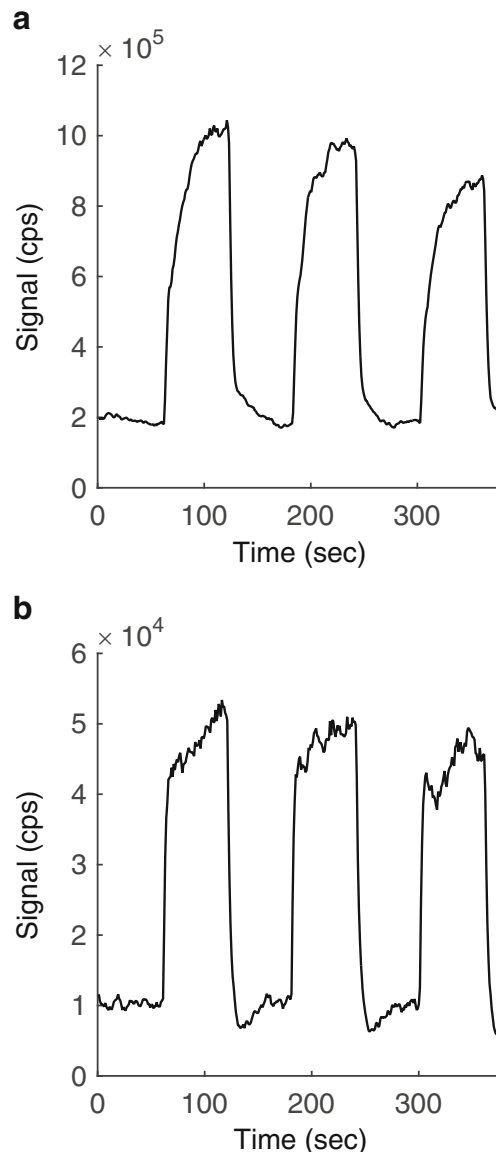

Figure 4. The results from the experiments in which gaseous analyte was introduced directly at the inlet for caffeine **(a)** and anthracene **(b)**. The support gas was changed every 60 s from argon to argon/hydrogen, starting with argon at time zero

signal from coumarin 460 from the glass slide is much larger than that observed in the gas phase, suggesting that the added hydrogen is changing the desorption process in addition to the ionization efficiency.

A variety of analytes have been tested with the argon-based discharges, both with hydrogen and without, and not all generated detectable signals. The tested analytes that were not detectable included cholesterol, benzo(a)pyrene, naphthalene, phenanthrene, perylene, and acenaphthene. Test analytes that generated signals included amitriptyline, nortriptyline, anthrone, acetanilide, xanthone, and nicotine. Generally speaking, the analytes that were successfully detected were nitrogen- or oxygen-containing compounds with relatively high proton affinities.

AC Discharge When using the AC discharge with argon and with gaseous analytes, an enhancement was observed that depended on the distance between the discharge outlet and the mass spectrometer inlet. When the discharge was placed 1 cm away from the inlet, the addition of hydrogen reduced the signal. However, at 2 cm away from the inlet, enhancement was seen similar to that obtained with the H_2/Ar DBD. At a distance of 3 cm from the inlet, the enhancement was not observed. The interplay among atmospheric entrainment, flow into the MS inlet, and gas-phase kinetics is affecting the ionization process in a manner that warrants further study.

With the addition of H_2 to the helium AC discharge, no signal enhancement could be seen regardless of the position of the discharge relative to the MS inlet. This led us to experiment with the electrical environment of the discharge to determine the effect it has on signal enhancement. These results are discussed later in the paper.

Changes to Analyte Ionization Mechanism

Potential Causes for [M]$^+$ Ion Signal Enhancement The mechanism by which M$^+$ ions are generated in the hydrogen-doped plasmas is still unclear. The creation of M$^+$ ions via charge transfer in pure helium discharges has been attributed to charge transfer with species such as N_2^+, NO$^+$, and O_2^+ [6, 25]. However, neither N_2^+ nor O_2^+ has been observed in great abundance in a pure argon discharge [8], and neither ion is in the mass range observable with our instrument. Within the range that we have observed ($\approx 35 < m/z < 110$), there are no changes in the background spectra that would account for the increase in sensitivity via charge transfer ionization with the addition of H_2 to the discharge. The relevant background spectra are included in the Supplemental Information as Figure S1.

Potential Causes of [M + H]$^+$ Ion Signal Enhancement The observed signal enhancement for [M + H]$^+$ peaks can most readily be attributed to an increase in proton donors in the plasma. As noted in the introduction, hydrogen added to noble gas plasmas leads to the formation of highly acidic H_3^+, ArH$^+$, and HeH$^+$ ions. Additional support for the formation of possible proton donors is found in a modeling study of an argon-hydrogen glow discharge by Bogaerts and Gijbels [26]. Relevant rate constants for H_2/Ar discharges are given in Table 3. Without a detailed model of gas mixing and of the kinetics of

reagent ion formation, it is impossible to say whether the ArH$^+$ and H_3^+ ions are protonating analyte ions directly or providing a more efficient path for the formation of protonated water clusters. Bogaerts and Gijbels did not include either water or nitrogen in their model, and both clearly are important for ADI sources, either as support gas contaminants or components of the atmosphere. The lack of fragmentation of analyte species argues against the highly acidic ions acting as the direct proton transfer reagents. The large difference between the proton affinity of H_3^+ and most analytes would lead to fragmentation of the analytes if H_3^+ were the proton transfer reagent [27, 28]. However, the background spectra, if one assumes that they are representative of what is seen by the analyte, argue against water clusters being the ultimate proton transfer reagents. In all cases, the addition of H_2 lowers the intensities of the water cluster peaks in the background spectra.

Some comparative number densities are useful in thinking about the effects of added hydrogen. Water is typically present in ultra-high purity helium and argon at a level below 1 ppm, or $\sim 3.4 \times 10^{13}$ molecules cm^{-3}. Atmospheric water is present at a density about 2.4×10^{17} cm^{-3}, but it is not present in the primary discharge. 2.9% H_2 corresponds to 7.1×10^{17} cm^{-3}. It is safe to assume that Ar-H_2 reactions are dominant in the primary discharge.

Clearly, the gas-phase chemistry of these systems is complex. We cannot, based on the experimental information available to us, assign a detailed ionization mechanism that accounts for the sensitivity increases that we observe.

Alternate Grounding Pathway

Our experimental results mentioned above indicated that the way the plasma was grounded significantly affected whether signal enhancement was observed or not. By grounding, we refer to whether the plasma is grounded to the needle electrode in the DBD, the inlet of the mass spectrometer, to the open air, or any combination of these. For instance, when using the He AC discharge, which is always grounded through the plate electrode, no signal enhancement was observed when using H_2/He as the plasma gas. However, when using the H_2/Ar AC discharge, signal enhancement was still observable. Based on these findings, we determined to provide a forced alternate grounding pathway for the DBD to see how the signal enhancement was affected.

For the He DBD, the grounded wire was placed 4 mm downstream from the DBD exit. Under these conditions, the visible plasma was attracted to the wire, and did not propagate beyond it. Experiments were conducted using gaseous caffeine and switching the plasma gas, but no signal enhancement was seen. Upon removal of the wire, and without changing the position of either the DBD or the gaseous caffeine outlet, the experiments were repeated and signal enhancement was observed as reported previously [9]. The experiment were repeated with the wire in place, but with voltage applied to the wire. Again, signal enhancement was not seen while either positive or negative bias was applied to the wire. The range of voltages

Table 3. Selected Reaction Rate Constants for Important Reactions in the Argon/Hydrogen plasma [12]

Chemical reaction	Rate constant
Ar$^+$ + H_2→ArH$^+$ + H	7.4×10^{-10} cm^3/s ± 25%
ArH$^+$ + H_2→H_3^+ + Ar	1.4×10^{-9} cm^3/s ± 100%
Ar$^+$ + H_2O→H_2O$^+$ + Ar	1.4×10^{-9} cm^3/s ± 25%
H_2O$^+$ + H_2O→products	1.7×10^{-9} cm^3/s ± 30%

applied was 0 to –100 V and 0 to +100 V in separate experiments. The capacitor used was rated only to 150 VDC, so higher voltages were not explored.

These experiments were repeated using the Ar DBD. In these cases, the wire was placed 1 mm downstream of the DBD exit because of the shorter plasma plume obtained when using argon as the support gas. When using the grounded wire, signal enhancement was still observed; although the overall signal intensity was lower by a factor of 2, and the enhancement when using H_2/Ar was two times instead of five as observed before. This could be due in part to the wire interrupting the gas flow towards the MS inlet. However, when the RC circuit was used, the signal enhancement was eliminated by applying a bias of only 25 V positive or negative.

We also observed that the signal enhancement decreased as we increased the voltage applied to the inlet of the mass spectrometer. The MicrOTOF II has an inlet voltage range of 500 to 6000 V. When set to 6000 V, a signal enhancement was still seen, but it was small compared with that seen at 500 V.

Background Ion Changes

DBD　The mass spectra of the background ions revealed that there are significant differences between the pure helium or argon discharges and the hydrogen-doped discharges. See the Supplemental Information Figure S1 for background mass spectra for the He and Ar DBD as well as the He AC discharge and their H_2-doped counterparts. Although the mass calibration of the mass spectrometer is good enough to identify many of the ions, not all were identified successfully. However, some general identification could be done based on what has been observed in other similar discharges [16, 29]. For both the pure argon and pure helium DBD, the predominant ions were protonated water clusters $(H(H_2O)_n^+)$. The most abundant ion in each case was the $n = 3$ water cluster, but the $n = 2, 4, 5$, and 6 ions were also observed. With the addition of hydrogen, in each case the abundance of all the water clusters decreased. The main water cluster ion remained the $n = 3$ ion, but its abundance was significantly smaller than in the pure-gas discharge. This could be due to the production of other species such as ArH^+, HeH^+, and H_3^+, but none of these were detected by the mass spectrometer. Both HeH^+ and H_3^+ were outside the available mass range. Assuming that almost all ArH^+ formed would quickly react to form H_3^+, it is reasonable that it would not show up in the mass spectra even though it was in the observable mass range.

Significant background ions in the spectra also included the $[M + H]^+$ ions of acetone, $CH_3CN(H_2O)$, $CH_3CN(CH_3OH)$, methyl acetate, and ethyl acetate. These are all solvents present in our laboratory, so were likely ionized from the lab air. Without MS/MS capability, the other background ions in the spectra were unidentifiable.

The background mass spectra with the addition of a grounded wire show significant changes for all gases used. The peaks corresponding to the water cluster ions were reduced dramatically. We have not successfully identified the peaks that appear instead of the water cluster ions. However, it is significant to note that the mass spectrum for the grounded pure helium DBD does not differ from that of the grounded H_2/He DBD. This is understandable considering that they yield signals of the same intensity—without any signal enhancement when using H_2/He. However, the background mass spectrum of the grounded, pure argon DBD did show differences from the grounded H_2/Ar DBD background spectrum. Again, we were unable to identify all the ions.

There were also significant differences between the background mass spectra obtained with the grounded H_2/Ar DBD and those obtained with voltage applied to the wire. These background spectra are shown in the Supplemental Information, Figure S2. These significant differences correspond to the loss of signal enhancement when the voltage is applied to the wire.

AC Discharge　The background spectra for the AC discharge included the protonated water clusters and many of the solvent-based ions recorded from the DBD. In addition, we identified a series of copper-containing ions: Cu^+, $CuNH_3^+$, $Cu(NH_3)_2^+$, $CuNH_3H_2O^+$, and $Cu(H_2O)_2^+$, presumably products of sputtering of the grounded copper end cap electrode. Of these ions, $CuNH_3H_2O^+$ was the most intense and was the base peak in both the He and H_2/He AC discharge background spectra. These two spectra were essentially the same, consistent with the lack of signal enhancement when using H_2/He as the plasma gas. Table S1 in the Supplemental Information section details the identification of copper-containing ions based on accurate masses.

Somewhat surprisingly, the intensities of the copper-containing ions were lower in the pure argon AC discharge than they were in either the He or H_2/He discharges. One would expect more efficient sputtering from more massive Ar ion than from He. However, the addition of H_2 to the Ar discharge changes the picture completely. The addition of H_2 to the Ar discharge increased the intensity of the $CuNH_3H_2O^+$ peak relative to the pure Ar discharge by factors of 4 to 30, depending on the distance between the ground electrode and the entrance to the mass spectrometer. This change is consistent with reported increases in sputtering efficiency with the addition of low percentages of H_2 to low-pressure Ar glow discharges [30]. The background spectra for the Ar AC discharges are included in the Supplemental Information as Figure S3.

The intensity of the $CuNH_3H_2O^+$ peak in the H_2/Ar AC discharge background spectra increased by more than an order of magnitude as the distance between source and inlet was increased from 1 to 3 cm. This dramatic change reemphasizes the strong dependence of plasma plume chemistry on position in the plume, and the importance of the relative positions of source, sample, and MS inlet in determining the effects of changes in plasma gas composition.

Absorption Measurements

As noted in the introduction, the grounds for the pin-to-ring DBD used in these experiments and for the similar LTP discharge are poorly defined. The discharge anchors itself readily
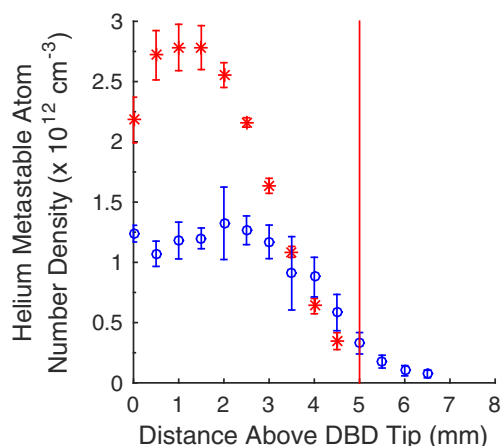
Figure 5. Absolute number densities of helium metastable atoms (He$_m$) in the helium DBD with and without a grounded wire in place. The red line shows the location of the wire when the grounded DBD measurements were taken. The point downstream from the wire was below the detection limit

to any conductor placed in the downstream volume and appears more robust to the naked eye. To provide a more quantitative measure of the effect of the added ground, we measured number densities of He$_m$ atoms at 0.5 mm intervals starting at the capillary exit and working downstream. Results are shown in Figure 5. The ground wire increased the He$_m$ density by a factor of ~2 between the capillary exit and the ground wire, but no He$_m$ atoms were detectable downstream from the wire. These observations suggest that the enhancing effect of H$_2$ on the He discharges requires the interaction of the analyte with an active discharge. There is no enhancement when a ground is placed upstream from the analyte or in the case of the AC discharge, in which only a weak afterglow comes in contact with the analyte.

In contrast, with an argon plasma gas, the enhancement is observable both with a grounding wire in place and with the AC discharge. The two plasma gases operate by different mechanisms.

Conclusions

We have demonstrated the enhancement in mass spectrometric signal obtained when using hydrogen-doped argon as the support gas in an ADI source compared with the signal obtained with the pure gas discharge. These positive results highlight the possibilities of using mixed gases in plasma-based ADI-MS. There is a wide variety of gas mixtures that could be tested to enhance the ionization efficiency when using plasma gases such as helium, argon, and nitrogen. More research is needed in this field to exploit the many potential advantages.

The lack of correlation between surface temperatures and signal levels suggest the contribution of a non-thermal desorption mechanism when using H$_2$/Ar as the plasma gas. Experiments with downstream grounds emphasize the complex nature of the interaction of the discharges, particularly the DBDs, with their surroundings. Their performance depends strongly

on the environment in which they are operated. The operating conditions of the mass spectrometer as well as interactions with conducting surfaces present while operating ADI plasma sources have significant effects on the signal enhancement with added H$_2$.

Acknowledgments

References

1. Takats, Z., Wiseman, J.M., Gologan, B., Cooks, R.G.: Mass spectrometry sampling under ambient conditions with desorption electrospray ionization. Science **306**, 471–473 (2004)
2. Cody, R.B., Laramée, J.A., Durst, H.D.: Versatile new ion source for the analysis of materials in open air under ambient conditions. Anal. Chem. **77**, 2297–2302 (2005)
3. Harper, J.D., Charipar, N.A., Mulligan, C.C., Zhang, X., Cooks, R.G., Ouyang, Z.: Low-temperature plasma probe for ambient desorption ionization. Anal. Chem. **80**, 9097–9104 (2008)
4. Andrade, F.J., Shelley, J.T., Wetzel, W.C., Webb, M.R., Gamez, G., Ray, S.J., Hieftje, G.M.: Atmospheric pressure chemical ionization source. 2. Desorption-ionization for the direct analysis of solid compounds. Anal. Chem. **80**, 2654–2663 (2008)
5. Na, N., Zhao, M., Zhang, S., Yang, C., Zhang, X.: Development of a dielectric barrier discharge ion source for ambient mass spectrometry. J. Am. Soc. Mass Spectrom. **18**, 1859–1862 (2007)
6. Venter, A.R., Douglass, K.A., Shelley, J.T., Hasman, G., Honarvar, E.: Mechanisms of real-time, proximal sample processing during ambient ionization mass spectrometry. Anal. Chem. **86**, 233–249 (2013)
7. Monge, M.E., Harris, G.A., Dwivedi, P., Fernández, F.M.: Mass spectrometry: recent advances in direct open air surface sampling/ionization. Chem. Rev. **113**, 2269–2308 (2013)
8. Chan, G.C.Y., Shelley, J.T., Jackson, A.U., Wiley, J.S., Engelhard, C., Cooks, R.G., Hieftje, G.M.: Spectroscopic plasma diagnostics on a low-temperature plasma probe for ambient mass spectrometry. J. Anal. At. Spectrom. **26**, 1434–1444 (2011)
9. Wright, J.P., Heywood, M.S., Thurston, G.K., Farnsworth, P.B.: The effects of added hydrogen on a helium atmospheric-pressure plasma jet ambient desorption/ionization source. J. Am. Soc. Mass Spectrom. **24**, 335–340 (2013)
10. Heywood, M.S., Taylor, N., Farnsworth, P.B.: Measurement of helium metastable atom densities in a plasma-based ambient ionization source. Anal. Chem. **83**, 6493–6499 (2011)
11. Albritton, D.L.: Ion-neutral reaction-rate constants measured in flow reactors through 1977. At. Data Nucl. Data **22**, 1–89 (1978)
12. Bedford, D.K., Smith, D.: Variable-temperature selected ion flow tube studies of the reactions of Ar$^+$, Ar^{+2}, and ArH^{+n} (n = 1–3) ions wi H$_2$, HD and D$_2$ at 300 K and 80 K. Int. J. Mass Spectrom. **98**, 179–190 (1990)
13. Eiden, G.C., Barinaga, C.J., Koppenaal, D.W.: Communication. Selective removal of plasma matrix ions in plasma source mass spectrometry. J. Anal. At. Spectrom. **11**, 317–322 (1996)
14. Koppenaal, D.W., Eiden, G.C., Barinaga, C.J.: Collision and reaction cells in atomic mass spectrometry: development, status, and applications. J. Anal. At. Spectrom. **19**, 561–570 (2004)
15. Rothwell, H.L., Amme, R.C., Van Zyl, B.: Excited hydrogen and argon atom production by charge transfer of metastable Ar$^+$ ions in H$_2$ molecules. J. Chem. Phys. **68**, 4326–4327 (1978)
16. McKay, K., Walsh, J.L., Bradley, J.W.: Observations of ionic species produced in an atmospheric pressure pulse-modulated RF plasma needle. Plasma Sources Sci. Technol. **22**, 035005 (2013)
17. Hunter, E.P.L., Lias, S.: Evaluated gas phase basicities and proton affinities of molecules: an update. J. Phys. Chem. Ref. Data **27**, 413–656 (1998)

18. Sung Lee, H., Drucker, M., Adams, N.G.: Thermal energy reactions of H_3^+ and H_3O^+ with a series of small organic molecules. Int. J. Mass Spectrom. **117**, 101–114 (1992)

19. Wròblewski, T., Ziemczonek, L., Karwasz, G.P.: Proton transfer reactions for ionized water clusters. Czech. J. Phys. **54**, C747–C752 (2004)

20. Hayen, H., Michels, A., Franzke, J.: Dielectric barrier discharge ionization for liquid chromatography/mass spectrometry. Anal. Chem. **81**, 10239–10245 (2009)

21. Wiley, J.S., Garcia-Reyes, J.F., Harper, J.D., Charipar, N.A., Ouyang, Z., Cooks, R.G.: Screening of agrochemicals in foodstuffs using low-temperature plasma (LTP) ambient ionization mass spectrometry. Analyst **135**, 971–979 (2010)

22. Reininger, C., Woodfield, K., Keelor, J.D., Kaylor, A., Fernández, F.M., Farnsworth, P.B.: Absolute number densities of helium metastable atoms determined by atomic absorption spectroscopy in helium plasma-based discharges used as ambient desorption/ionization sources for mass spectrometry. Spectrochim. Acta B **100**, 98–104 (2014)

23. Hanley, D.C., Harris, J.M.: Quantitative dosing of surfaces with fluorescent molecules: characterization of fractional monolayer coverages by counting single molecules. Anal. Chem. **73**, 5030–5037 (2001)

24. Jackson, A.U., Garcia-Reyes, J.F., Harper, J.D., Wiley, J.S., Molina-Diaz, A., Ouyang, Z., Cooks, R.G.: Analysis of drugs of abuse in biofluids by low temperature plasma (LTP) ionization mass spectrometry. Analyst **135**, 927–933 (2010)

25. Shelley, J.T., Wiley, J.S., Chan, G.C.Y., Schilling, G.D., Ray, S.J., Hieftje, G.M.: Characterization of direct-current atmospheric-pressure discharges useful for ambient desorption/ionization mass spectrometry. J. Am. Soc. Mass Spectrom. **20**, 837–844 (2009)

26. Bogaerts, A., Gijbels, R.: Hybrid Monte Carlo—fluid modeling network for an argon/hydrogen direct current glow discharge. Spectrochim. Acta B **57**, 1071–1099 (2002)

27. Herman, J.A., Harrison, A.G.: Effect of reaction exothermicity on the proton transfer chemical ionization mass spectra of isomeric C_5 and C_6 alkanols. Can. J. Chem. **59**, 2125–2132 (1981)

28. Herman, J.A., Harrison, A.G.: Effect of protonation exothermicity on the chemical ionization mass spectra of some alkylbenzenes. Org. Mass Spectrom. **16**, 423–427 (1981)

29. Brüggemann, M., Karu, E., Hoffmann, T.: Critical assessment of ionization patterns and applications of ambient desorption/ionization mass spectrometry using FAPA-MS. J. Mass Spectrom. **51**, 141–149 (2016)

30. Laidani, N., Bartali, R., Tosi, P., Anderle, M.: Argon-hydrogen rf plasma study for carbon film deposition. J. Phys. D Appl. Phys. **37**, 2593–2606 (2004)